

New approach to design a compact triband bandpass filter using a multilayer structure

Sohrab MAJIDIFAR^{1,*}, Mohsen HAYATI²

¹Young Researchers and Elite Club, Kermanshah Branch, Islamic Azad University, Kermanshah, Iran

²Department of Electrical Engineering, Kermanshah Branch, Islamic Azad University, Kermanshah, Iran

Received: 14.09.2016

Accepted/Published Online: 17.02.2017

Final Version: 05.10.2017

Abstract: In this paper, a triband bandpass filter is presented using a dual-layer structure. Three H-shaped resonators are utilized in the proposed structure. The first and third resonators are placed at the top and bottom layers, respectively. The second resonator is divided into two parts: one half is on the top and the other half is at the bottom. The effective permittivity at the first and second layers is different, resulting in different resonant frequencies. The fabricated triband bandpass filter operates at 5.44/6.98/8.36 GHz, with fractional bandwidths of 6.6%/6%/2.9% and measured minimal insertion losses of 1.9/1.7/2 dB.

Key words: Triband, multilayer structure, passband tuning

1. Introduction

Microstrip filters are in high demand in modern communication systems due to their significant features such as compactness, planar structure, and ease of fabrication [1–21]. Multistandard communication systems require multiband microwave filters. A variety of approaches to designing microstrip triband bandpass filters (BPF) have been proposed [4–21]. Combining three single-band filters in parallel has been presented in [4]. In this approach, each passband can be independently controlled, while the circuit size is not compact enough. Asymmetric stepped-impedance resonators (SIRs) with only one discontinuity can also be used to construct multiband BPFs with the merit of compact circuit size, low loss, and better design feasibility [5–8]. Creating a transmission zero to split one passband of a dual-band BPF into two has been presented in another approach [9]. This method achieves a controllable isolation between passbands, whereas the transition bands are not sharp. Half-wavelength [10] and quarter-wavelength [11] SIRs have been utilized to design quadband or triband BPFs. The trisection SIRs have been used to design triband filters in [12,13]. Another type of triband BPFs has been designed using multimode resonators [14] such as stepped-impedance resonators or stub-loaded resonators [15–18]. Using the higher modes of a dual-mode resonator has been reported in [19]. High performance and compact size triband bandpass filters have been proposed using high-temperature superconducting structure [20] and defected ground structure [21], respectively.

In this paper, a triband BPF is presented using a simple principle: different dielectric constant results in different resonant frequencies. This hypothesis is tested by using a multilayer configuration. In order to reduce the physical size and increase the isolation between passbands, the surface-coupling structure is modified

*Correspondence: sohrab.majidi@gmail.com

to coupling between the layers in the proposed dual-layer structure. Using the proposed structure has two important advantages: reduction of physical size (almost 50%) and reduction of designer limitations through access to the two substrates in a single structure. To validate the proposed method, a triband BPF prototype has been designed, fabricated, and measured.

2. Filter design

The basic structure of the proposed triband bandpass filter and its simulation results are shown in Figures 1a and 1b, respectively. The dimensions of this structure, which is composed of three cascaded H-shaped resonators, are as follows: $a = 0.176$ mm, $b = 2.9$ mm, $c = 2.37$ mm, $d = 6.77$ mm, $e = 0.176$ mm, $h = 5.17$ mm, $i = 3$ mm, $m = 1.17$ mm, and $n = 0.7$ mm. The proposed structure was designed on RT/duroid 5880 with a dielectric constant of 2.2 and a thickness of 0.381 mm. As illustrated in Figure 1b, the resonant frequencies of the basic structure have been centered at 6.38 GHz, 6.88 GHz, and 7.4 GHz. There is no isolation between the passbands; hence, passband control is not possible. Figure 2 shows the circuit model of the basic structure.

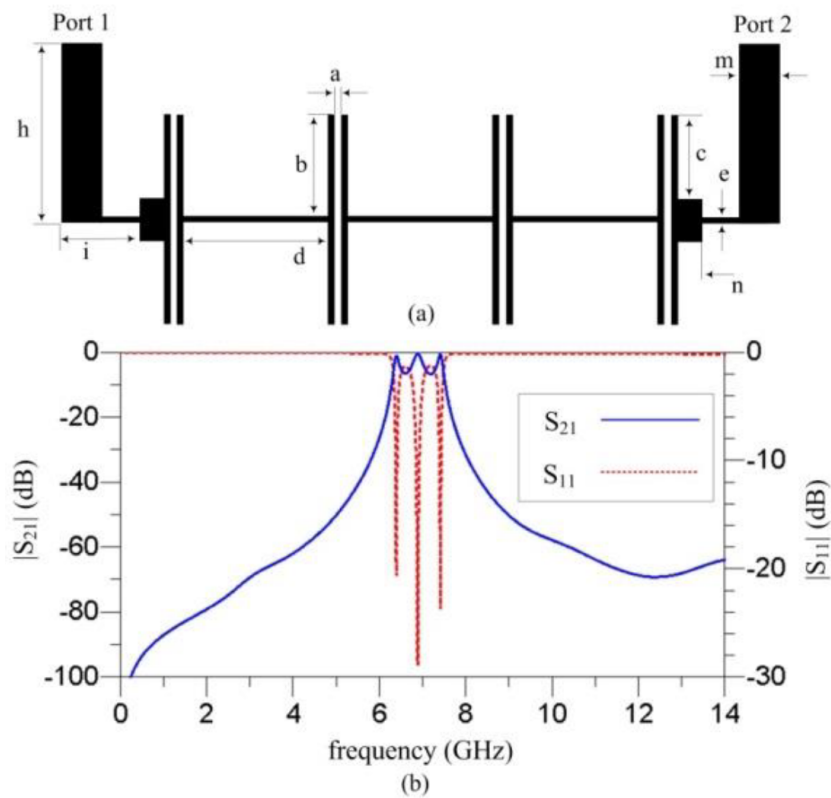


Figure 1. Basic structure of the proposed triband bandpass filter: a) layout, b) simulation results.

In this model, L_i and C_i are inductance and capacitance of input and output ports, respectively. C_1 and C_2 introduce the body capacitance of the vertical lines in the H-shape resonator. C_g is the coupling capacitance between vertical lines and L_1 shows the inductance of the horizontal line in the H-shape resonator. Using Eqs. (1)–(5) and certain optimization [2], these circuit parameters are calculated as follows: $L_i = 1$ nH, $C_i = 0.61$

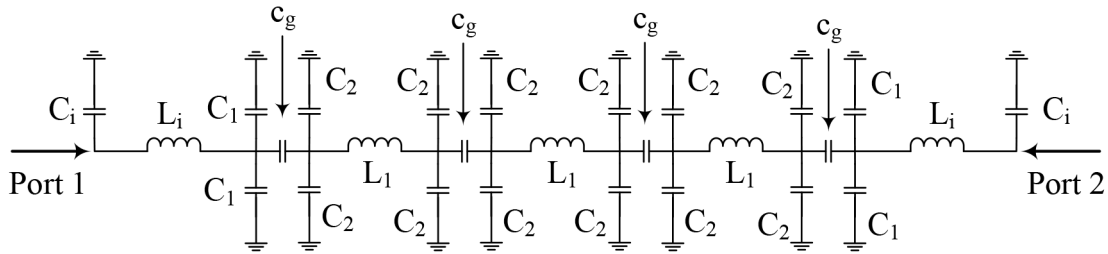


Figure 2. Circuit model of the basic structure.

pF, $L_1 = 3.87$ nH, $C_1 = 0.12$ pF, $C_2 = 0.11$ pF, and $C_g = 0.073$ pF.

$$C = [8.85(10)^{-12} \left\{ \left[\frac{\epsilon_r w}{h} \right]^{1.08} + [2\pi \left(\frac{\epsilon_r + 1}{2} \right) \left(\frac{1}{\ln(\frac{8h}{w} + 1)} - \frac{w}{8h} \right)]^{1.08} \right\}^{0.926}] l \quad (1)$$

$$L = \frac{l z_c}{v_p} \quad (2)$$

$$v_p = \frac{c}{\sqrt{\epsilon_{re}}} \quad (3)$$

For $w/h \leq 1$

$$\epsilon_{re} = \frac{\epsilon_r + 1}{2} + \frac{\epsilon_r - 1}{2} \left\{ \left[1 + 12 \frac{h}{w} \right]^{-0.5} + 0.04 \left[1 - \frac{w}{h} \right]^2 \right\}, \quad z_c = \frac{\eta}{2\pi \sqrt{\epsilon_{re}}} \ln \left[8 \frac{h}{w} + 0.25 \frac{w}{h} \right] \quad (4)$$

For $w/h \geq 1$

$$\epsilon_{re} = \frac{\epsilon_r + 1}{2} + \frac{\epsilon_r - 1}{2} \left[1 + 12 \frac{h}{w} \right]^{-0.5}, \quad z_c = \frac{\eta}{\sqrt{\epsilon_{re}}} \left\{ \frac{w}{h} + 1.393 + 0.677 \ln \left[\frac{w}{h} + 1.444 \right] \right\}^{-1}, \quad (5)$$

where the equivalent capacitance and inductance of the resonator parts are introduced by C and L, z_c and v_p characteristics impedance and phase velocity, respectively, w , l , h , and ϵ_{re} are line width, line length, substrate thickness, and effective permittivity, respectively, η is a constant equal to $120\pi\Omega$, and c represents the light speed.

Figure 3 shows the EM and circuit simulation results of the basic structure and its model. As shown in Figure 3, this result is well matched with the EM simulation results.

To control the passbands and increase the isolation between them, a dual layer structure is used. In this method, the proposed basic structure in Figure 1a is divided into two parts. The first resonator and half of the second resonator remain unchanged on the top layer. The next half of the second resonator and the third resonator are displaced from the top to the bottom layer, while the back of the bottom layer is metalized as the ground plane. The input/output ports are assembled between the top layer/bottom layer and the ground plane. The substrate thickness of the first resonator is double of a single layer and its effective permittivity is 1.7, while the effective permittivity of the third resonator is 2.2. Two parts of the second resonator, which are designed on the top and bottom layers, are connected through a via hole and resonate between the resonant frequencies of the first and third resonators.

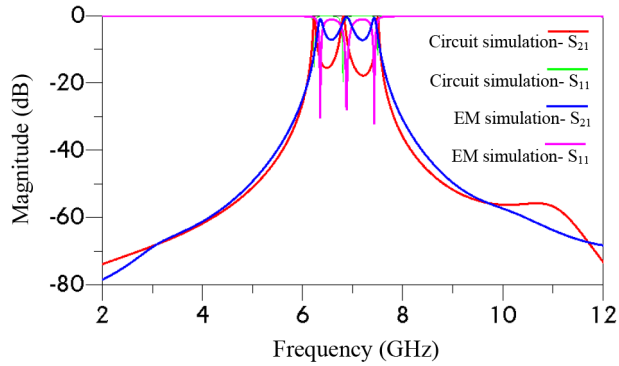


Figure 3. EM and circuit simulation results of the basic structure and its model.

Figures 4a and 4b show the layout and simulation results of the proposed filter. As illustrated in Figure 4a, the dimensions of the resonators on the bottom layer have been scaled to control the passband frequencies. Input and output lines are designed on both sides of the filter to be connected to 50- Ω SMA. The resonant frequencies of the filter appear at 5.33 GHz, 6.88 GHz, and 8.27 GHz. The first passband is created by the third resonator on the bottom layer due to increasing the scale of the third resonator, while the associated effective dielectric constant remains unchanged and equals 2.2.

The second band is related to the second resonator, whose two parts (on the top and bottom layer) are connected with a via hole. The third band is created by the first resonator on the top layer, where the effective dielectric constant is no longer 2.2, but has changed to 1.7. This smaller effective permittivity shifts the resonant frequency to higher frequencies. Hence, three fully tunable passbands are realized.

To improve passband isolation, two deep transmission zeros have been located at 6.07 GHz and 7.58 GHz with magnitudes of -35 dB and -42 dB, respectively. Two out-of-band transmission zeros at 4.75 GHz and 8.68 GHz have been generated to realize sharp passband skirt performance. The simulation results of the proposed filter in terms of insertion loss, return loss, and sharpness are shown in Table 1. Total size of the fabricated filter without feed lines is $0.34 \lambda_g \times 0.16 \lambda_g$, where λ_g is the guided wavelength of the first passband. A comparison between the total size of the filters (both in this work and in those reported in the introduction) is shown in Table 2.

Table 1. Passbands specifications of the designed filter.

Passband	Insertion loss (dB)	Return loss (dB)	Sharpness of the first/second transition band of each passband (dB/GHz)
First	0.32	15	58.62/37.78
Second	0.39	16.65	36.17/43.59
Third	0.52	22.4	34.69/85

Table 2. Comparison between the total size of the filters.

Ref. no.	[4]	[7]	[9]	[11]	[12]	[13]	[14]
Total size ($\lambda_g \times \lambda_g$)	0.32×0.49	0.33×0.25	0.181×0.176	0.108×0.521	0.195×0.195	0.24×0.22	0.16×0.17
Ref. no.	[15]	[16]	[17]	[18]	[20]	[21]	This work
Total size ($\lambda_g \times \lambda_g$)	0.26×0.13	0.17×0.15	0.26×0.22	0.18×0.38	0.066×0.051	0.14×0.22	0.16×0.34

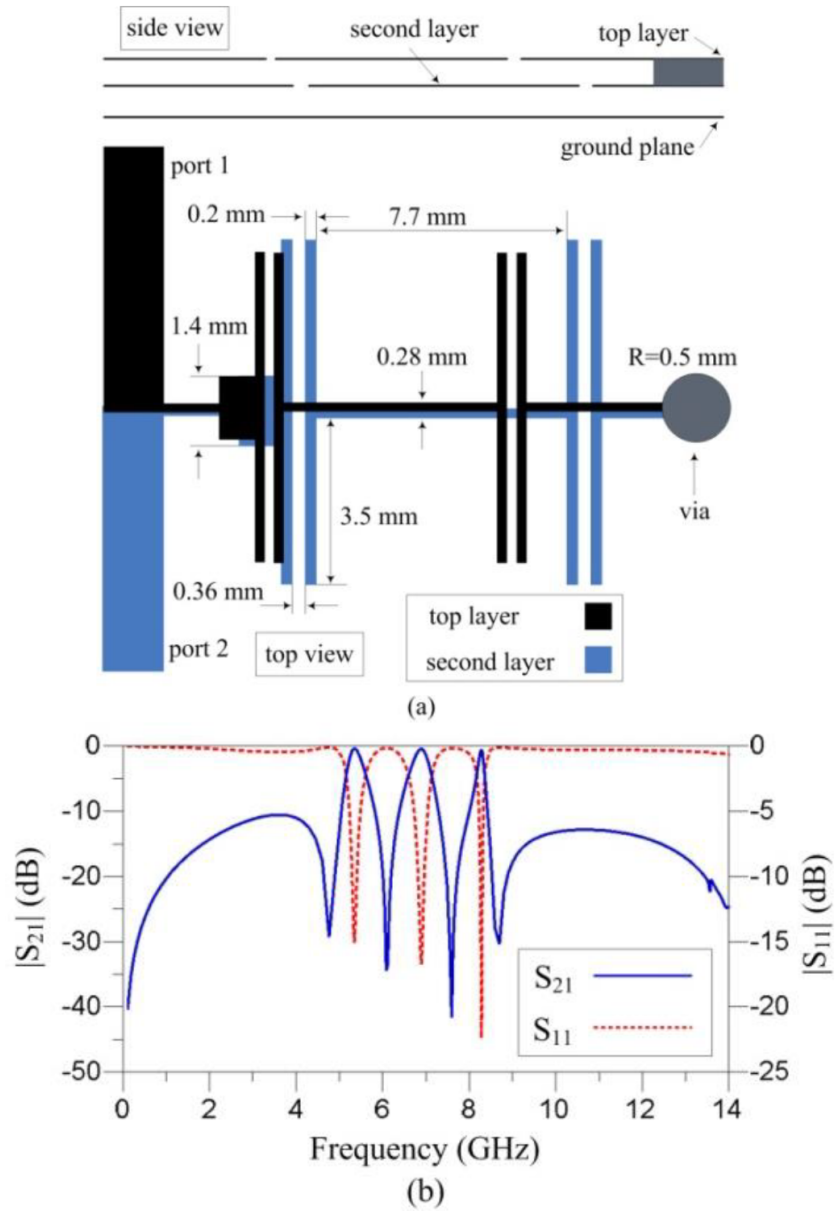


Figure 4. Proposed triband bandpass filter: a) layout, b) simulation results.

3. Fabrication and measurement

Figure 5 shows the pictures of the top layer, bottom layer, and final filter structure. The measurement and simulation results of the filter are shown in Figure 6. The triband BPF operates at 5.44/6.98/8.36 GHz, with fractional bandwidths of 6.6%/6%/2.9% and measured minimal insertion losses of 1.2/1.7/2 dB. Compared to the simulation result, the measurement result shows a 110-MHz, 100-MHz, and 90-MHz frequency shift for the first, second, and third passbands, respectively. This shift is mainly due to the gap between the two connected layers (top and bottom layer), which is neglected in the simulation.

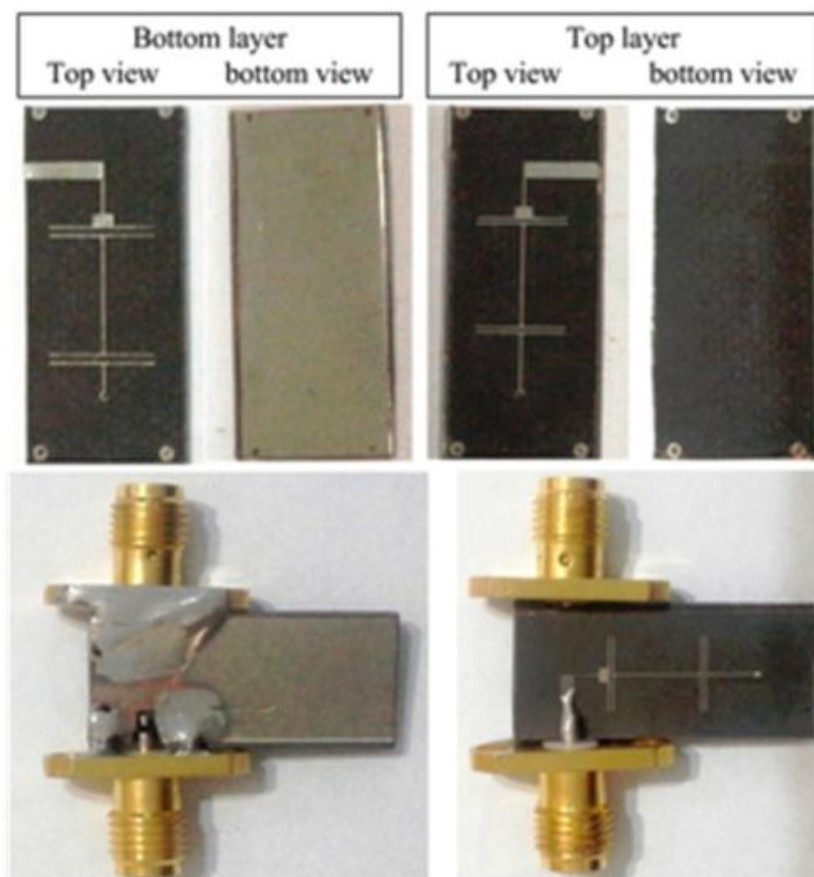


Figure 5. Pictures of the fabricated filter.

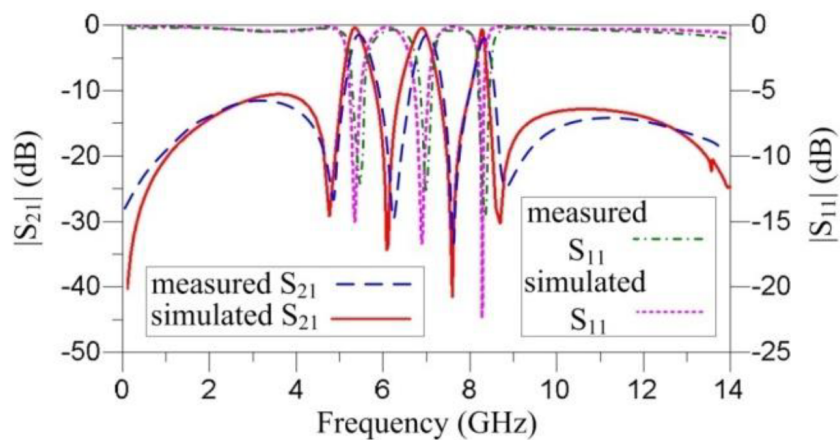


Figure 6. Simulation and measurement results of the proposed filter.

4. Conclusion

A compact adjustable triband bandpass filter is presented in this paper. In the presented approach, two stacked layers of substrate are used to introduce two different effective permittivities to control the multiple resonant frequencies. In this structure, each band can be independently controlled, which makes the proposed triband filter suitable for multiband wireless communication systems.

References

- [1] Demirel S, Uyank C. Design and analysis of a novel UWB bandpass filter using 3-D EM simulation-based neural network model with HSA. *Turk J Elec Eng & Comp Sci* 2016; 3: 656-668.
- [2] Majidifar S. High performance microstrip LPFs using dual taper loaded resonator. *Optik* 2016; 127: 3484-3488.
- [3] Majidifar S. Design of high performance miniaturized lowpass filter using new approach of modeling. *Appl Comput Electrom* 2016; 31: 52-57.
- [4] Song F, Wei B, Zhu L, Feng Y, Wang R, Cao B. A novel tri-band superconducting filter using embedded stub-loaded resonators. *IEEE T Appl Supercon* 2016; 26: 1502009.
- [5] Chang YC, Kao CH, Weng MH, Yang RY. Design of the compact dual-band bandpass filter with high isolation for GPS/WLAN applications. *IEEE Microw Wirel Co* 2009; 19: 780-782.
- [6] Wu HW, Yang RY. A new quad-band bandpass filter using asymmetric stepped impedance resonators. *IEEE Microw Wirel Co* 2011; 21: 203-205.
- [7] Chen WY, Weng MH, Chang SJ, Kuan H, Su YH. A new tri-band bandpass filter for GSM, WiMAX and ultra-wideband responses by using asymmetric stepped impedance resonators. *Prog Electromagn Res* 2012; 124: 365-381.
- [8] Weng MH, Kao CH, Chang YC. A compact dual-band bandpass filter with high band selectivity using cross-coupled asymmetric SIRs for WLANs. *J Electromagnet Wave* 2010; 24: 161-168.
- [9] Ren LY. Tri-band bandpass filters based on dual-plane microstrip/DGS slot structure. *IEEE Microw Wirel Co* 2010; 20: 429-431.
- [10] Yang CF, Chen YC, Kung CY, Lin JJ, Sun TP. Design and fabrication of a compact quad-band bandpass filter using two different parallel positioned resonators. *Prog Electromagn Res* 2011; 115: 159-172.
- [11] Zhang S, Zhu L. Compact tri-band bandpass filter based on $\lambda/4$ resonators with U- folded coupled-line. *IEEE Microw Wirel Co* 2013; 23: 258-260.
- [12] Chu QX, Lin XM. Advanced triple-band bandpass filter using tri-section SIR. *Electron Lett* 2008; 44: 295-296.
- [13] Chen FC, Chu QX. Compact triple-band bandpass filter using pseudo interdigital trisection stepped impedance resonators. *Microw Opt Techn Lett* 2008; 50: 2462-2465.
- [14] Li Q, Zhang YH, Feng X, Fan Y. Tri-band filter with multiple transmission zeros and controllable bandwidths. *Int J Microw Wirel Technol* 2016; 8: 9-13.
- [15] Lan SW, Wen MH, Chang SJ, Hung CY, Liu SK. A tri-band bandpass filter with wide stopband using asymmetric stub-loaded resonators. *IEEE Microw Wirel Co* 2015; 25: 19-21.
- [16] Wei F, Qin PY, Guo YJ, Shi XW. Design of multi-band bandpass filters based on stub loaded stepped-impedance resonator with defected microstrip structure. *IET Microw Antenna P* 2015; 10: 1-7.
- [17] Wu Q, Cui H, Sun P, Sun H, Sun X. On-chip tri-band bandpass filters using square ring open-stub loaded resonator on GaAs substrate. *Microw Opt Technol Lett* 2016; 58: 1958-1961.
- [18] Wei F, Guo YJ, Qin PY, Shi XW. Compact balanced dual- and tri-band bandpass filters based on stub loaded resonators. *IEEE Microw Wirel Co* 2015; 25: 76-78.
- [19] Luo S, Zhu L, Sun S. Compact dual-mode triple-band bandpass filters using three pairs of degenerate modes in a ring resonator. *IEEE T Microw Theory* 2011; 59: 1222-1229.
- [20] Liu H, Ren B, Zhan X, Guan X, Wen P, Zhu S, Peng Y, Ma Z. Tri-band high-temperature superconducting bandpass filters using multimode resonators. *IEEE T Microw Theory* 2016; 26: 1501506.
- [21] Wei F, Qin PY, Guo YJ, Ding C, Shi XW. Compact balanced dual- and tri-band BPFs based on coupled complementary split-ring resonators (C-CSR). *IEEE Microw Wirel Co* 2016; 26: 107-109.